Counter-Rotating Accretion Disks

R.V.E. Lovelace

Department of Astronomy, Cornell University, Ithaca, NY 14853

Tom Chou

Laboratory of Atomic and Solid State Physics, Cornell University, Ithaca, NY 14853

ABSTRACT

We consider accretion disks consisting of counter-rotating gaseous components with an intervening shear layer. Configurations of this type may arise from the accretion of newly supplied counter-rotating gas onto an existing co-rotating gas disk. For simplicity we consider the case where the gas well above the disk midplane is rotating with angular rate $+\Omega$ and that well below has the same properties but is rotating with rate $-\Omega$. Using the Shakura-Sunyaev alpha turbulence model, we find self-similar solutions where a thin (relative to the full disk thickness) equatorial layer accretes very rapidly, essentially at free-fall speed. As a result the accretion speed is much larger than it would be for an alpha disk rotating in one direction. Counter-rotating accretion disks may be a transient stage in the formation of counter-rotating galaxies and in the accretion of matter onto compact objects.

Subject headings: accretion disks - counter-rotating galaxies

1.   INTRODUCTION

The widely considered models of accretion disks have gas rotating in one direction with a turbulent viscosity acting to transport angular momentum outward (Shakura & Sunyaev 1973). However, recent observations point to more complicated disk structures in both active galactic nuclei and on a galactic scale. Warped and tilted nuclear accretion disks have been detected for example in NGC 4753 (Steinman-Cameron et al. 1992). Recent high spectral resolution studies of normal galaxies has revealed counter rotating gas (Ciri, Bettoni, & Galleta 1995) and/or stars in many galaxies of all morphological types - ellipticals, spirals, and irregulars (see reviews by Rubin 1994 and Galletta 1996). NGC 4826 (Braun et al. 1994) and IC 1459 (Franx & Illingworth 1988) are examples of galaxies with central counter-rotating gas and stellar disks, respectively. In elliptical galaxies, the counter-rotating component is usually in the nuclear core and may result from merging of galaxies with opposite angular momentum. Newly supplied gas with misaligned angular momentum in the nuclear region of a galaxy may have important consequences for nuclear activity if there is a rotating massive black hole at the galaxy's center (Scheuer 1992). In contrast, in a number of spirals and S0 galaxies, counter-rotating disks of stars and/or gas have been found to co-exist with the primary disk out to large distances $(10-20\,\mathrm{kpc})$, with the first example, NGC 4550, discovered by Rubin, Graham, and Kenney (1992). It is not likely that the large scale counter-rotating disks result from mergers of flat galaxies with opposite angular momenta because of the large vertical thickening observed in simulation studies of such mergers (Barnes 1994). Thakar and Ryden (1996) discuss different possibilities, (a) that the counter-rotating matter comes from the merger of an oppositely rotating gas rich dwarf galaxy with an existing spiral, and (b) that the accretion of gas occurs over the lifetime of the galaxy with the more recently accreted gas counter-rotating. Subsequent star formation in the counter-rotating gas may then lead to counter-rotating stars. The two-stream instability between counter-rotating gas and co-rotating stars may enhance the rate of gas accretion (Lovelace, Jore, & Haynes 1996).

An important open problem is how counter-rotating gas disks form and what their structures are on galactic scales and on the scale of disks in active galactic nuclei. Here, we investigate accretion disks consisting of counter-rotating gaseous components with gas at large z rotating with angular rate $+\Omega(r)$ and gas at large negative z rotating at rate $-\Omega(r)$. The interface between the components at $z \sim 0$ constitutes a supersonic shear layer and is shown in Figure 1.
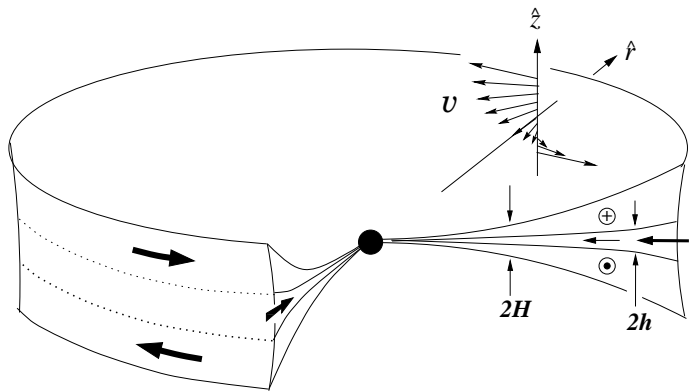

Fig. 1.— Structure of two apposed, counter-rotating accretion disks and the midplane boundary layer. The inset shows the three dimensional view of the velocity field for the $n = 1/2$ case shown in Figure 2. The velocity variation is analogous to that in the Ekman layer of a rotating fluid (such as the ocean) where the Coriolis force balances the viscous force (Batchelor 1967).

Configurations of this type may exist in astrophysical settings such as halo-disk interactions and the accretion of newly supplied counter-rotating gas onto an existing co-rotating disk. It might at first be supposed that powerful Kelvin-Helmholtz instabilities heat the gas to escape speed and rapidly destroy the assumed config-

uration. However, supersonic shear layers exist and exhibit gross stability in stellar and extragalactic jets (Hardee, Cooper, & Stone 1994). In the counter-rotating disk, matter approaching the equatorial plane from above and below has angular momenta of opposite signs with the result that there is angular momentum annihilation at $z = 0$, the matter loses its centrifugal support and accretes at essentially free-fall speed. On the other hand, accretion disks rotating in one direction are modeled assuming a turbulent viscosity which is crucial for the outward transport of angular momentum (Shakura & Sunyaev 1973). The counter-rotating disks can also be expected to be turbulent owing in part to the Kelvin-Helmholtz instability, and turbulent viscosity can transport angular momentum outward in the large $|z|$ regions of the disk.

2. THEORY AND SELF-SIMILAR SOLUTIONS

For stationary, axi-symmetric disk-like flows in cylindrical coordinates (r, ϕ, z) with

$$\mathbf{v} = [v_r(r,z), v_\phi(r,z), v_z(r,z)], \qquad (1)$$

the momentum and continuity equations are

$$(\mathbf{v}\cdot\nabla)v_r = \frac{v_\phi^2}{r} - \frac{1}{\rho}\frac{\partial p}{\partial r} + g_r + \nu_\perp \frac{\partial^2 v_z}{\partial z^2} + \nu_\parallel \frac{\partial}{\partial r}\left[\frac{\partial v_r}{\partial r} + \frac{v_r}{r}\right] \tag{2}$$

$$(\mathbf{v}\cdot\nabla)v_\phi = \frac{-v_r v_\phi}{r} + \nu_\perp \frac{\partial^2 v_\phi}{\partial z^2} + \nu_\parallel \frac{\partial}{\partial r}\left[\frac{\partial v_\phi}{\partial r} + \frac{v_\phi}{r}\right] \tag{3}$$

$$(\mathbf{v}\cdot\nabla)v_z = -\frac{1}{\rho}\frac{\partial p}{\partial z} + g_z + \nu_\parallel \left[\frac{\partial^2 v_z}{\partial r^2} + \frac{1}{r}\frac{\partial v_z}{\partial r}\right] + \nu_\perp \frac{\partial^2 v_z}{\partial z^2} \tag{4}$$

$$\frac{1}{r}\frac{\partial}{\partial r}\left(r\rho v_r\right) + \frac{\partial}{\partial z}\left(\rho v_z\right) = 0. \tag{5}$$

Here, $\rho(r,z)$ is the gas density, $p(r,z)$ is the pressure, $\mathbf{g} = -\nabla\Phi$ is the gravitational acceleration

with $\Phi(r, z)$ the potential. For simplicity, terms involving the gradient of the dynamic viscosity $(\rho\nu)$ have been neglected. Because the microscopic viscosity is negligible for the conditions considered, we assume ν arises from small scale turbulence and can be approximated by the "alpha" prescription of Shakura and Sunyaev (1973) as $\nu = \alpha c_s H$, where H is the full half-thickness of the disk which is assumed thin ($H \ll r$), c_s is the isothermal sound speed, and α is a dimensionless constant much less than unity. Since the turbulent motions may not be isotropic, we allow two different tensor components of ν ($\nu_\parallel$ for shear in the $\hat{r} - \hat{\phi}$ direction and $\nu_\perp$ for shear in the vertical direction) with possible different $r-$dependences. We also assume the second viscosity coefficient $\nu' = \frac{2}{3}\nu$ so that the stress tensor $T_{ij} = \rho v_i v_j + p\delta_{ij} + T_{ij}^\nu$ with the viscous contribution $T_{ij}^\nu = -\nu(\partial v_i/\partial x_j + \partial v_j/\partial x_i)$. Here, $\nu = \nu_\perp$ if $j = z$, and $\nu = \nu_\parallel$ otherwise, yielding equations (2)-(4).

We seek self-similar solutions to equations (2)-(5) of the form

$$v_r(r, z) = -u_r(\zeta)V_c(r),$$

$$v_\phi(r, z) = u_\phi(\zeta)V_c(r),$$

$$v_z(r, z) = -\left(\frac{h(r)}{r}\right)u_z(\zeta)V_c(r), \tag{6}$$

$$\rho(r, z) = \rho_0(r)Z\left(\frac{z}{H(r)}\right),$$

where $\zeta \equiv z/h(r)$ is the dimensionless vertical distance in the disk with $h(r)$ a length scale identified subsequently, and $V_c(r) = [r(\partial\Phi/\partial r)|_{z=0}]^{1/2}$ is the circular velocity of the gas. The potential is due in general to disk and halo matter and a central object. Here and subsequently we neglect the pressure force in the radial equation of motion. We consider cases where $V_c(r) = (GM/r_0)^{1/2}(r_0/r)^n$, with r_0 a constant length scale. The value $n = 1/2$ corresponds to a Keplerian disk around an object of mass M, and

3

$n = 0$ to a flat rotation curve applicable to flat galaxies.

Substitution of equation (6) into equations (2) and (3) gives

$$(1 + \epsilon^2\eta^2\zeta^2)u_r'' = u_\phi^2 + nu_r^2 - 1 + \eta\zeta u_r u_r'$$
$$-u_z u_r' - \epsilon^2\zeta\eta(\eta + 2n)u_r' + \epsilon^2(1 - n^2)u_r, \quad (7)$$

$$(1 + \epsilon^2\eta^2\zeta^2)u_\phi'' = (n - 1)u_r u_\phi - u_z u_\phi'$$
$$+\eta\zeta u_r u_\phi' - \epsilon^2\zeta\eta(\eta + 2n)u_\phi' + \epsilon^2(1 - n^2)u_\phi, \quad (8)$$

where a prime denotes a derivative with respect to ζ. We have chosen the scaling such that $\nu_\perp r/(V_c h^2) \equiv 1$ and $\epsilon^2 \equiv \nu_\parallel/rV_c$, and defined $\eta \equiv (r/h)(dh/dr)$. We assume that the disk is not strongly self-gravitating and that it is vertically isothermal so that its overall half-thickness is $H \sim (c_s/V_c)r$ which is the same as for a disk rotating in one direction. From the assumed scaling, $h^2 = \nu_\perp r/V_c$, and an assumed alpha viscosity prescription $\nu_\parallel = \alpha c_s H$ and $\nu_\perp = \alpha c_s h$ (Regev 1983), $\delta \equiv h/H \sim \alpha \ll 1$. As a result, (4) simplifies to $(\partial_z p) = -\rho\partial_z\Phi$. which determines the isothermal density profile $Z(\zeta) = \exp(-\delta^2\zeta^2)$. From the assumed scaling $\rho_0(r) \propto r^{-\beta-1/2}$, equation (5),

$$u_z' = \left[\beta + n - \frac{1}{2} - 2\delta^2\zeta^2\left(\frac{r}{H}\frac{dH}{dr}\right)\right]u_r$$
$$+\eta\zeta u_r' + 2\delta^2\zeta u_z, \quad (9)$$

determines v_z. For consistency of the self-similar solutions, ϵ must be independent of r, implying $\eta = 1$ and $(r/H)(dH/dr) = 1$ if the viscosities scale similarly, $\nu_\perp \sim \nu_\parallel$.

Equations (7)-(9) constitute a closed system for the dimensionless functions $u_r(\zeta)$, $u_\phi(\zeta)$, and $u_z(\zeta)$. Applying equations (7)-(9) to the flow suggested in Figure 1 1, we infer that $u_r(\zeta)$ is an even function of ζ, while $u_\phi(\zeta)$ and $u_z(\zeta)$ are odd functions. For $|\zeta| \gg 1$, we impose $u_r \simeq (1 + n)\epsilon^2$

and $u_\phi \simeq \pm\sqrt{1 - (n + 1)^2\epsilon^4}$ so as to have $u_r'' \to 0$ and $u_\phi'' \to 0$. These limits correspond to an α disk rotating in one direction far away from the $\zeta = 0$ midplane. For $n = 1/2$, $u_r(\zeta \gg 1) \simeq 3\epsilon/2$ and $v_r(\zeta \gg 1) = 3\nu_\parallel/2r$, agreeing with the radial velocity of a single thin Keplerian disk with viscosity $\nu_\parallel = \epsilon^2 rV_c$.

A steady counter-rotating disk may result from gas continuously supplied at large r. Similarly, steady state solutions where gas is entrained and delivered vertically onto the faces of the disk may exist. We assume that $v_z\rho(r, z) \to 0$ as $|z| \to \infty$. Considering only this subset of solutions, we demand the accretion rate

$$\dot{M} = 2\pi\int_{-\infty}^{\infty} dz r\rho(r, z)|v_r(r, z)| \simeq 2\pi r\rho_0(r)$$
$$\times V_c(r)h(r)\int_{-H/h}^{H/h} d\zeta u_r(\zeta)e^{-\delta^2\zeta^2}, \quad (10)$$

be a constant. A sufficient condition for this is $\beta = \eta - n + 1/2$ and $\delta = h/H$ is r-independent. For an alpha disk rotating in one direction, $\dot{M}_{SS} = 2\pi r\Sigma|v_r|_{SS}$, with the accretion speed $|v_r|_{SS} \sim \alpha c_s H/r \ll c_s$, where $\Sigma = \int dz\rho$ is the disk's surface mass density (Shakura & Sunyaev 1973). In contrast, for a counter-rotating disk equation (10) gives $\dot{M}_{CR} = 2\pi r\Sigma|v_r|_{cr}$, with accretion speed (averaged over z) $|v_r|_{CR} \sim (h/H)V_c$. For the same α, we have $|v_r|_{CR} \gg |v_r|_{SS}$: the accretion speed of the counter-rotating disk is much larger than that of the disk rotating in one direction.

A further constraint on solutions of equations (2)-(5) is obtained by considering the energy dissipation and radiation of the disk. The viscous dissipation per unit area of the disk is

$$D(r) = \int_{-H}^{H} dz\,\rho\,\nu\left[2\left(\frac{\partial v_r}{\partial r}\right)^2 + \left(r\frac{\partial\Omega}{\partial r}\right)^2\right.$$
$$\left.+2\left(\frac{\partial v_z}{\partial z}\right)^2 + \left(\frac{\partial v_z}{\partial r} + \frac{\partial v_r}{\partial z}\right)^2 + \left(\frac{\partial v_\phi}{\partial z}\right)^2\right], \quad (11)$$

where $\Omega = v_\phi/r$. For a disk rotating in one

4

direction, the dominant contribution to $D(r)$ is from the $\partial\Omega/\partial r$ term and this gives $D_{SS}(r) \approx \Sigma\nu_\parallel(n+1)^2(V_c/r)^2 = \dot{M}_{SS}(V_c/r)^2(n+1)^2/(3\pi)$. In contrast, for a counter-rotating disk, the dominant contributions are from the terms $\partial v_r/\partial z$ and $\partial v_\phi/\partial z$ with the result

$$D_{CR}(r) \simeq \Sigma\nu_\perp V_c^2/(hH)$$
$$\sim \dot{M}_{CR}(V_c/r)^2/(3\pi) \sim (r/H)^2 D_{SS}(r). \quad (12)$$

The dissipated energy is radiated from the faces of the disk if it is optically thick in the z-direction and thus $D = 4acT^4/(3\kappa\Sigma)$, where a is the radiation constant, c the speed of light, κ the opacity, and T is the internal disk temperature. For the general scaling $\kappa \propto \rho^a T^b$, the counter-rotating disk thus has $T \propto r^{-\xi}$ with $\xi = (3+2a+n)/(4-b+a/2)$ and $h \propto T^{1/2}r^{1+n} \propto r^\eta$. For example, for Kramer's opacity $a = 1,\ b = -3.5$, we have $\xi = (5+n)/8$ and $\eta = (11+15n)/16$, whereas for electrons scattering opacity $a = 0,\ b = 0$, and $\xi = (3+n)/4$ and $\eta = (11+9n)/8$. In general, the strict requirement $\eta = 1$ for our self-similar solutions will not be satisfied, but this is not expected to be important if $\epsilon \ll 1$ (see Figure 2)[1]. The apparent surface temperature of the disk $T_{eff}(r)$ is given by $D(r) = 2\sigma T_{eff}^4$, where $\sigma = ac/4$ is the Stefan-Boltzmann constant. The dependence for the counter-rotating disk, $T_{eff} \propto r^{-(n+1)/2}$, is the same as for an alpha disk rotating in one direction. Similarly, the spectrum, F_ω, obtained by integrating the Planck function $B_\omega(T_{eff}(r))$ over the surface area of the disk, $F_\omega \propto \omega^{(3n-1)/(n+1)}$, is the same as for a disk rotating in one direction. For an optically thin disk, $D = 2H\Lambda$, where $\Lambda(\rho, T)$ is the emissivity of the disk matter.

In the limit $\epsilon = \delta = 0$ and $\beta = \eta - n + 1/2$, equation (9) gives $u_z = \eta\zeta u_r$, which reduces

---

[1] Because the viscosity scaling $\nu_\perp \sim \nu_\parallel$ implies $\eta = 1$, values of $\eta \neq 1$ are strictly consistent with our scalings and constant $\dot{M}$ only if the turbulent viscosity is anisotropic such that shear perpendicular to the plane is governed by $\nu_\parallel = \epsilon^2 rV_c \sim r^{1-n}$, but shear in the plane is determined by $\nu_\perp = h^2V_c/r \sim r^{2\eta-n-1}$.

equations (7) and (8) to $u_r'' = u_\phi^2 + nu_r^2 - 1$ and $u_\phi'' = (n-1)u_r u_\phi$, respectively. These have the integral

$$(u_\phi')^2 - \frac{1-n}{2}(u_r')^2 + (1-n)u_r u_\phi^2$$
$$+ \frac{n(1-n)}{3}u_r^3 - (1-n)u_r = \text{const.} \quad (13)$$

Evaluating (13) at $\zeta = 0$ and $\zeta = \infty$ gives $[u_\phi'(0)]^2 = (1-n)u_r(0) - n(1-n)u_r^3(0)/3$. We utilize this result by first finding the single independent initial condition $u_r(0)$ for $\delta = \epsilon = 0$, then allow $\delta,\ \epsilon \neq 0$, and perturbatively find the proper values of $u_r(0)$ and $u_\phi'(0)$. Three of five initial conditions are fixed by symmetry: $u_r'(0) = u_\phi(0) = u_z(0) = 0$. We search for solutions by tuning $u_r(0)$ and $u_\phi'(0)$, regarding ϵ and δ as fixed. In principle, the required values $u_r(\infty)$ and $u_\phi(\infty)$ are satisfied for a range of δ. The additional parameter $\delta \gg \epsilon$ can be chosen according to the behavior of $u_z(\infty)$ desired. Thus, a class of solutions exist located on curved segments in $[u_r(0), u_\phi'(0), \delta]$ space.

Figure 2 shows solutions to equations (7)-(9) for $\epsilon = 0.01$ and $\delta = 0.1$, corresponding to $h/H \simeq 1/10$ and $h/r \simeq 1/300$. Both Keplerian ($n = 1/2,\ \beta = 1$) and galactic ($n = 0,\ \beta = 3/2$) solutions are shown. The solutions are sensitive to the precise values of $u_r(0),\ u_\phi'(0),\ \delta$, and ϵ. Note that for $3 \lesssim |\zeta| \lesssim 7$, the solutions have a region with $u_r < 0$ indicating spiraling outflows on both sides of the midplane. The vertical velocities $v_z/V_c \ll u_r$ or u_ϕ are indistinguishable from the x-axis on the scale of Fig. 2. For large ζ, the density fall off gives $\rho v_z \to 0$.

3. DISCUSSION

Counter-rotating gas supplied to the outer part of an existing co-rotating gas disk will increase the mass accretion rate. Comparing accretion rates of a standard α-disk ($\dot{M}_{SS}$) with that of a counter-rotating Keplerian disk ($\dot{M}_{CR}$) of the same Σ and $\dot{M}$, we find from equation
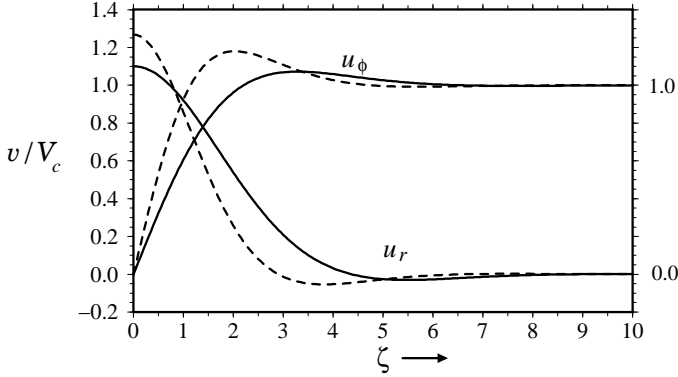
5

Fig. 2.— Solutions to Equations (2), (3), and (5) for $\epsilon = 0.01$ and $\delta = 0.1$ as a function of $\zeta = z/h(r)$. Solid lines correspond to a Keplerian disk ($n = 1/2, \beta = 1$) with $u_r(0) = 1.10007597\ldots$ and $u'_\phi(0) = 0.66260669\ldots$. The dashed curves correspond to $n = 0$ (flat rotation curve potential) and $\beta = 3/2$ and have initial values $u_r(0) = 1.26728681248\ldots$ and $u'_\phi(0) = 1.1256582571\ldots$. These values are close to those of the $\delta = \epsilon = 0$ "zero-order" solutions: $u_r(0) = [u'_\phi(0)]^2 = 1.100112673\ldots$ ($n = 1/2$) and $u_r(0) = [u'_\phi(0)]^2 = 1.2672806222\ldots$ ($n = 0$). All solutions reach their asymptotic values for $\zeta \to \infty$ and the vertical velocity $v_z/V_c \approx 0$ on this scale. Note that the midplane infall velocity for the Keplerian case is shear-reduced by a factor ~ 0.77 from the free-fall speed $(2GM/r)^{1/2}$.

(10) $\dot{M}_{CR}/\dot{M}_{SS} \simeq 1 + 0.58(\delta/\epsilon^2)$. For the values of Figure 2 this ratio is $\simeq 580$.

Thermal and/or dynamical instabilities may destroy the counter-rotating accretion flows described above. The relative importance of thermal and dynamical instabilities can be estimated by comparing the thermal dissipative time scale, $\tau_Q \approx \Sigma c_s^2/D_{CR}(r) \simeq (r/h)(H/V_c)(c_s/V_c)^2$, with dynamical and viscous time scales, $\tau_z \equiv h/c_s$, $\tau_\perp \equiv r/V_c$, and $\tau_\nu \equiv r^2/\nu_\perp$. We find $\tau_Q \sim \epsilon^2\delta^{-3}\tau_z \sim \epsilon^2\delta^{-5/2}\tau_\perp \sim \epsilon^4\delta\tau_\nu$. For $\epsilon = 0.01$ and $\delta = 0.1$, the thermal dissipation time $\tau_Q \ll \tau_z < \tau_\perp \ll \tau_\nu$. In contrast to the standard $\alpha-$disk, thermal equilibrium is maintained on time scales of possible flow instabilities of the inner shear layer. The Kelvin-

Helmholtz instabilities are likely to be the most important (Ray & Ershkovich 1983 and Choudhury & Lovelace 1984). If the counter-rotating disk is treated as a vortex sheet, then a local stability analysis indicates unstable warping for wave numbers $|k_\phi/k_r| < \sqrt{2}(c_s/\Omega r) \ll 1$.

Accretion of counter rotating gas by an existing co-rotating gas disk may be a transient stage in the formation of counter-rotating galaxies and in the accretion of matter onto rotating black holes in active galactic nuclei. We find that newly supplied counter-rotating gas drags inward the old co-rotating gas with an equal mass of old and new gas accreting rapidly. Thus the old co-rotating gas may be entirely "used up" (dragged to the center of a galaxy or into a black hole) if the mass of newly supplied gas exceeds that of the old gas disk. Accretion onto the faces of an existing thin disk may not have the symmetry shown in Figures 1 and 2.
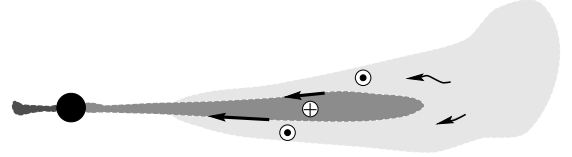

Fig. 3.— Schematic drawing of accretion of newly supplied counter-rotating gas ($\odot$) induced by viscous interaction with an existing disk of co-rotating gas ($\oplus$).

There may instead be two layers of rapid radial inflow bounding the existing gas disk near the midplane as sketched in Figure 3. Solutions for this configuration can be composed from those of Figure 2 if $h \ll H$.

REFERENCES

Barnes, J. E. 1992, ApJ, 393, 484

Batchelor, G. K. 1967, *An Introduction to Fluid Dynamics*, (Cambridge University Press: Cambridge), p. 197 Oosterloo, T. 1991, MNRAS, 248, 544

Braun, R., Walterbos, R. A. M., Kennicutt, R. C., and Tacconi, L. J. 1994, ApJ, 420, 558

Choudhury, S. R., and Lovelace, R. V. E. 1984, ApJ, **302**, 188.

Ciri, R., Bettoni, D., and Galletta, G. 1995, Nature, **375**(6533), 661.

Franx, M., and Illingworth, G. 1988, ApJ, 327, L55

Hardee, P. E., Cooper, M. A., Clarke, D. A., 1994, ApJ, **424**, 126

Lovelace, R.V.E., Jore, K.P., and Haynes, M. P. 1996, submitted to Astrophysical Journal

Ray, T. P., and Ershkovich, A. I. 1983, MNRAS, **204**, 821.

Regev, O. 1983, A&A, **126**, 146.

Rubin, V. C., Graham, J. A., and Kenney, J. D. P. 1992, ApJ, **394**(1), L9

Scheuer, P. A. G. 1992, in *Extragalactic Radio Sources: From Beams to Jets*, J. Roland, H. Sol, and G. Pelletier, eds., (Cambridge University Press: Cambridge), p. 368

Shakura, N. I. and Sunyaev, R. A. 1973, A& A., **24**,337.

Steinman-Cameron, T. Y., Kormendy, J., and Durisen, R. H. 1992, Astron. J., **104**(4), 1339

Thakar, A. R., and Ryden, B. S. 1996, in press, ApJ.